J. Fluid Mech. (1999), *vol.* 384, *pp.* 159–182. Printed in the United Kingdom

Solute transport in divergent radial flow through heterogeneous porous media

By PETER INDELMAN[1] AND GEDEON DAGAN[2]

[1] Faculty of Civil Engineering, Technion – Israel Institute of Technology, Technion City, Haifa 32000, Israel

[2] Department of Fluid Mechanics and Heat Transfer, Faculty of Engineering, Tel Aviv University, Ramat Aviv, 69978 Tel Aviv, Israel

(Received 16 November 1997 and in revised form 3 November 1998)

Radial flow takes place in a heterogeneous porous formation of random and stationary log-conductivity $Y(\boldsymbol{x})$, characterized by the mean $\langle Y \rangle$, the variance σ_Y^2 and the two-point autocorrelation ρ_Y which in turn has finite and different horizontal and vertical integral scales, I and I_v, respectively. The steady flow is driven by a head difference between a fully penetrating well and an outer boundary, the mean velocity U being radial. A tracer is injected for a short time through the well envelope and the thin plume spreads due to advection by the random velocity field and to pore-scale dispersion. Transport is characterized by the mean front $r = R(t)$ and by the second spatial moment of the plume S_{rr}. Under ergodic conditions, i.e. for a well length much larger than the vertical integral scale, S_{rr} is equal to the radial fluid trajectory variance X_{rr}.

The aim of the study is to determine $X_{rr}(t)$ for a given heterogeneous structure and for given pore-scale dispersivities. The problem is more complex than the similar one for mean uniform flow. To simplify it, the well is replaced by a line source, the domain is assumed to be infinite and a first-order approximation in σ_Y^2 is adopted. The solution is still difficult, being expressed with the aid of a few quadratures. It is found, however, that it can be derived quite accurately for a sufficiently small anisotropy ratio $e = I_v/I$ by retaining only one term of the velocity two-point covariance. This major simplification leads to simple calculations and even to analytical solutions in the absence of pore-scale dispersion.

To compare the results with those prevailing in homogeneous media, apparent and equivalent macrodispersivities are defined for convenience.

The major difference between transport in radial and uniform flow is that the asymptotic, large-time, apparent macrodispersivity in the former is smaller by a factor of 3 than in the latter. For a three-dimensional point source the reduction is by a factor of 5. This effect is explained by the rapid change of the mean velocity during the period in which the velocities of two particles injected at the source become uncorrelated.

In contrast, the equivalent macrodispersivity tends to its value in uniform flow far from the well, where the flow is slowly varying in space.

1. Introduction

We consider transport of a plume of an inert solute by water flowing through natural, large-scale, porous formations (aquifer, reservoir). Such formations are as a rule heterogeneous, their hydraulic conductivity K varying in space in an irregular manner and by orders of magnitude. This spatial variability causes enhanced spreading of solutes, with 'macrodispersion' coefficients much larger than those associated with pore-scale heterogeneity.

Following the common approach, we regard $K(\boldsymbol{x})$ as a RSF (random space function), to account for its erratic variation and uncertainty. As a result, the flow and transport variables are RSF as well. Modelling of transport is carried out in two steps: first, solving the flow equations and deriving the fluid velocity statistical moments; subsequently, the transport equation is solved in order to determine the solute concentration $C(\boldsymbol{x}, t)$ of a moving plume. The concentration field can be characterized locally in terms of the statistical moments of C: the ensemble mean $\langle C \rangle$, the variance σ_C^2, and higher moments. Alternatively, the plume may be characterized globally with the aid of spatial or temporal moments. For the sake of simplicity, we focus the present study on characterization by spatial moments.

In the past, considerable effort has been invested in solving transport under conditions of uniform mean flow (see e.g. Dagan 1989), that pertains to natural gradient flows, and mathematical models of transport have been developed. Thus, the average Darcy's law was shown to have a local structure with effective properties depending only on the medium structure, and second moments of flow variables have been derived in many cases of interest. Transport has been investigated experimentally by carefully conducted field tests, by computer simulations and theoretically by adopting approximations that led to simple, analytical solutions. The theoretical approach and a few relevant results are reviewed in §3.

There are important applications, however, in which the mean flow varies rapidly in space. We refer to wells that inject or pump water carrying a solute. Such problems arise for instance in injection of contaminants, in protection zones of pumping wells, in remediation schemes etc.

Non-uniform flows in heterogeneous media have been studied to a much lesser extent than the uniform ones (Shvidler 1966, 1985; Dagan 1982; Adams & Gelhar 1992; Desbarats 1992; Neuman & Orr 1993; Indelman & Abramovich 1994; Indelman 1996). It was shown that the constitutive equation (average Darcy's law) for non-uniform flow has a non-local structure and the effective conductivity is given by a convolution operator over the space. The approach developed in these studies allows statistical moments of flow variables to be derived. Thus, a few such moments were investigated by Indelman, Fiori & Dagan (1996) and Fiori, Indelman & Dagan (1998) and their results serve as background for the present study.

The problem here is to determine the spreading pattern of the solute, as affected by the random variation of $K(\boldsymbol{x})$. Field studies (Molz *et al.* 1986; Yeh *et al.* 1995) have demonstrated that the permeability spatial variability is indeed the dominating factor in solute dispersion. In spite of its importance, to the best of our knowledge there are no theoretical investigations of this topic in the literature, which deal exclusively with the effect of pore-scale dispersion, pertaining to homogeneous media (see e.g. Gelhar & Collins 1971; Dagan 1971; Chen 1987; Hsieh 1986; Valocchi 1986). This state of affairs is understandable in view of the complexity of the problem, of the numerical difficulties and of the fact that even the simpler case of transport in uniform flow has been investigated only recently.

The objective of the present study is to investigate advective transport for steady and diverging radial flow, pertaining to injecting wells. We derive approximate, simple, solutions that may help in understanding this important class of processes and may also serve for analysing field tests, for prediction purposes and for validating numerical codes. We also hope that the methodology developed here may prove useful for solving similar problems in other branches of environmental fluid mechanics.

The plan of the paper is as follows. After stating the general mathematical problem in § 2, we review briefly transport in uniform flow in § 3, with emphasis on results relevant to radial flow. Subsequently, in § 4, we introduce the various approximations that lead to a simple solution of transport in radial flow and conclude with a few applications in § 5.

2. Mathematical statement of the flow and transport problems

2.1. *General*

A porous formation lies in a domain Ω, of boundary $\partial\Omega$. The equations of flow are Darcy's law and the continuity equation

$$\boldsymbol{q} = -K\nabla H, \quad \nabla \cdot \boldsymbol{q} = 0 \tag{1}$$

where $\boldsymbol{q}$ is the specific discharge and H is the pressure head. With $\boldsymbol{x}(x_1, x_2, x_3)$ a Cartesian coordinate, $K(\boldsymbol{x})$ is modelled as a stationary RSF characterized by the statistical moments of $Y = \ln K$. Thus, $\langle Y \rangle = \ln K_G$ and $C_Y(\boldsymbol{x}', \boldsymbol{x}'') = \langle Y'(\boldsymbol{x}')\, Y'(\boldsymbol{x}'') \rangle = \sigma_Y^2\, \rho_Y(\boldsymbol{x}' - \boldsymbol{x}'')$, where $Y' = Y - \langle Y \rangle$ is the fluctuation. The geometric mean K_G, the variance σ_Y^2 and the autocorrelation ρ_Y are assumed to be given. If the usual assumption of log-normality is adopted, these moments define completely the structure.

Elimination of $\boldsymbol{q}$ in (1) leads to

$$\nabla^2 H + \nabla Y \cdot \nabla H = 0 \quad (\boldsymbol{x} \in \Omega) \tag{2}$$

which has to be solved with boundary conditions of given H or $\boldsymbol{q}$, assumed time independent, on $\partial\Omega$.

Once (2) is solved, the velocity field of the steady flow is given by $\boldsymbol{V}(x) = -\boldsymbol{q}/n = K\,\boldsymbol{E}/n$, where $n = \text{const}$ is the porosity and the notation $\boldsymbol{E} = -\nabla H$ is adopted for brevity. The velocity $\boldsymbol{V}$ serves as input to the transport problem, which is stated next.

The concentration C is defined as mass of tracer per volume of fluid. Then the transport equation is as follows:

$$\frac{\partial C}{\partial t} + \boldsymbol{V} \cdot \nabla C = \nabla \cdot (\boldsymbol{D}_d \cdot \nabla C) \quad (\boldsymbol{x} \in \Omega), \tag{3}$$

$$C(\boldsymbol{x}, 0) = C_0 \quad (\boldsymbol{x} \in \boldsymbol{V}_0), \quad C(\boldsymbol{x}, 0) = 0 \quad (\boldsymbol{x} \notin \boldsymbol{V}_0),$$

where $\boldsymbol{D}_d$ is the pore-scale dispersion tensor. The initial condition in (3) is of instantaneous injection of given C_0 in a volume $\boldsymbol{V}_0$. We follow here the Lagrangian approach in solving the transport problem (see e.g. Dagan 1989). The solution of (3) is expressed with the aid of the trajectories $x = \boldsymbol{X}_t(t; \boldsymbol{a}) = \boldsymbol{X}(t; \boldsymbol{a}) + \boldsymbol{X}_d(t)$, solutions of

$$\frac{\mathrm{d}\boldsymbol{X}}{\mathrm{d}t} = \boldsymbol{V}(X_t), \quad \frac{\mathrm{d}\boldsymbol{X}_d}{\mathrm{d}t} = \boldsymbol{w}_d(t), \quad \boldsymbol{X}(0) = \boldsymbol{a}, \quad \boldsymbol{X}_d(0) = 0 \quad (a \in \boldsymbol{V}_0). \tag{4}$$

In (4) $\boldsymbol{w}_d$ stands for a Wiener process, representing the velocity field associated with a Brownian motion type of transport, such that $\langle \boldsymbol{w}_d \rangle = 0$ and formally $\langle w_{di}(t') w_{dj}(t + t') \rangle = 2D_{dij}\delta(t)$. It follows that the displacement $\boldsymbol{X}_d$ is stationary and normal, with $\langle \boldsymbol{X}_d \rangle = 0$ and with covariance $\boldsymbol{X}_{dij}(t)$.

The solution of (3) can be written conveniently in the form

$$C(\boldsymbol{x}, t) = \int_{\boldsymbol{V}_0} C_0(\boldsymbol{a}) \delta[\boldsymbol{x} - \boldsymbol{X}_t(t; \boldsymbol{a})]\, \mathrm{d}\boldsymbol{a}. \tag{5}$$

Equation (5) may constitute the starting point for a numerical particle tracking solution. Indeed, with $\mathrm{d}M_0 = n\,C_0\,\mathrm{d}\boldsymbol{a}$ regarded as the mass of a material point in $\boldsymbol{V}_0$ and $\mathrm{d}M = n\int C\,\mathrm{d}\boldsymbol{x}$ its mass at time t, (5) states that the particle moves at $\boldsymbol{X}_t$, with conservation of mass ($\mathrm{d}M_0 = \mathrm{d}M$).

Equation (5) may serve for computing the local moments $\langle C\rangle$, $\sigma_C^2, \ldots$ or the plume spatial or temporal moments in terms of the statistics of $\boldsymbol{X}_t$. For the sake of simplicity we choose the characterization by the spatial moments that are defined as follows:

$$\left.\begin{aligned} M &= \int n\,C\,\mathrm{d}\boldsymbol{x}, \;\; \boldsymbol{R}(t) = \frac{1}{M}\int n\,\boldsymbol{x}\,C\,\mathrm{d}\boldsymbol{x}, \\ S_{ij}(t) &= \frac{1}{M}\int n\,(\boldsymbol{x}_i - R_i)\,(\boldsymbol{x}_j - R_j)C\,\mathrm{d}\boldsymbol{x}, \end{aligned}\right\} \tag{6}$$

where $\boldsymbol{R}$ is the plume centroid and S_{ij} $(i, j = 1, 2, 3)$ are its second spatial moments. We here limit the study to large V_0 at the heterogeneity scale, permitting us to adopt the ergodic hypothesis with regard to the random variables (6), i.e. to exchange them with their ensemble mean. Then substituting (5) in (6) and averaging yields

$$\left.\begin{aligned} \boldsymbol{R} \approx \langle\boldsymbol{R}\rangle &= \frac{n}{M}\int_{V_0}\langle C_0(\boldsymbol{a})\,\boldsymbol{X}(t;\boldsymbol{a})\rangle\,\mathrm{d}\boldsymbol{a}, \\ \boldsymbol{S}_{ij} \approx \langle S_{ij}\rangle &= \frac{n}{M}\int_{V_0}\langle C_0(\boldsymbol{a})\,(X_{ti} - R_i)(X_{tj} - R_j)\rangle\,\mathrm{d}\boldsymbol{a}. \end{aligned}\right\} \tag{7}$$

The advantage of characterizing the plume by the spatial moments (7) is that they depend directly on the moments of the trajectories, which can be determined in turn by robust approximations (see § 2.2). Besides, they depend weakly on pore-scale dispersion under the usual conditions of high Péclet number encountered in applications (see e.g. Naff 1990; Fiori 1996).

The derivatives $\boldsymbol{U} = \mathrm{d}\boldsymbol{R}/\mathrm{d}t$ and $D_{ij} = \frac{1}{2}\mathrm{d}S_{ij}/\mathrm{d}t$ define the plume mean velocity and apparent 'macrodispersion' coefficients, respectively, whereas in conditions of mean uniform flow $\alpha_{ij} = D_{ij}/U$ are 'macrodispersivities' (see discussion in § 4.4).

Hence, solving the transport problem reduces to determining the moments of the trajectories (4), given the log-conductivity structure, the pore-scale dispersion tensor and head boundary conditions. An approximate procedure to achieve this goal is discussed next.

2.2. *First-order approximation*

Both flow and transport problems are difficult to solve exactly. Numerical methods and Monte Carlo simulations have been used in the past (see § 3), but they are affected by numerical errors and are computer demanding.

Approximate, simple, results were obtained in the past by adopting a first-order approximation in σ_Y^2 (see e.g. Dagan 1989). Thus the head field is expanded in an asymptotic sequence $H = H^{(0)} + H^{(1)} + \cdots$ with $H^{(0)} = O(1)$, $H^{(1)} = O(\sigma_Y), \ldots$ and similarly $\boldsymbol{E} = -\nabla H$. Substituting in (2) and expanding yields

$$\nabla^2 H^{(0)} = 0, \quad \nabla^2 H^{(1)} = \nabla Y \cdot \boldsymbol{E}^{(0)}. \tag{8}$$

Furthermore, $H^{(0)}$ satisfies the head boundary conditions on $\partial\Omega$, whereas $H^{(1)}$ obeys homogeneous ones. Thus, $H^{(0)}$ is the solution of the flow problem in a homogeneous formation, whereas $H^{(1)}$ satisfies a Poisson equation with a random forcing term depending on $\boldsymbol{E}^{(0)} = -\nabla H^{(0)}$ and the same is true for higher-order terms.

The velocity field has the expansion

$$\boldsymbol{V}(\boldsymbol{x}) = \frac{1}{n} K\, \boldsymbol{E} = \frac{1}{n} K_G\, \mathrm{e}^{Y'} (\boldsymbol{E}^{(0)} + \boldsymbol{E}^{(1)} + \cdots)$$
$$= \frac{1}{n} K_G\, (\boldsymbol{E}^{(0)} + Y' \boldsymbol{E}^{(0)} + \boldsymbol{E}^{(1)}) + O(\sigma_Y^2). \tag{9}$$

With $\boldsymbol{V} = \boldsymbol{U} + \boldsymbol{u}$, where $\boldsymbol{U} = \langle \boldsymbol{V} \rangle$, we get from (9) at first order

$$\boldsymbol{U} = \frac{K_G}{n} \boldsymbol{E}^{(0)} + O(\sigma_Y^2), \quad \boldsymbol{u} = \frac{K_G}{n} (Y' \boldsymbol{E}^{(0)} + \boldsymbol{E}^{(1)}) + O(\sigma_Y^2). \tag{10}$$

This leads to the following expressions for the velocity two-point covariances:

$$u_{ij}(\boldsymbol{x}', \boldsymbol{x}'') = \left(\frac{K_G}{n} \right)^2 [E_i^{(0)}(\boldsymbol{x}')\, E_j^{(0)}(\boldsymbol{x}'')\, C_Y(\boldsymbol{x}', \boldsymbol{x}'') + E_i^{(0)}(\boldsymbol{x}')\, C_{E_j Y}(\boldsymbol{x}'', \boldsymbol{x}')$$
$$+ E_j^{(0)}(\boldsymbol{x}'') C_{E_i Y}(\boldsymbol{x}', \boldsymbol{x}'') + C_{E_i E_j}(\boldsymbol{x}', \boldsymbol{x}'')] \tag{11}$$

where $C_{E_j Y}(\boldsymbol{x}', \boldsymbol{x}'') = \langle Y'(\boldsymbol{x}'')\, E_j^{(1)}(\boldsymbol{x}') \rangle$ and $C_{E_i E_j}(\boldsymbol{x}', \boldsymbol{x}'') = \langle E_i^{(1)}(\boldsymbol{x}')\, E_j^{(1)}(\boldsymbol{x}'') \rangle$ and neglected terms in (11) are $O(\sigma_Y^4)$. Thus, the velocity mean and covariance are expressed in terms of those of the zero- and first-order approximations of the head gradient.

Finally, after expanding $\boldsymbol{X}_t = \langle \boldsymbol{X} \rangle + \boldsymbol{X}' + \boldsymbol{X}_d$ in the argument of $\boldsymbol{V} = \boldsymbol{U} + \boldsymbol{u}$ in (4), the trajectories satisfy at leading order the equations

$$\frac{\mathrm{d}\langle \boldsymbol{X}_t \rangle}{\mathrm{d}t} = \frac{\mathrm{d}\langle \boldsymbol{X} \rangle}{\mathrm{d}t} = \boldsymbol{U}(\langle \boldsymbol{X} \rangle), \quad \frac{\mathrm{d}\boldsymbol{X}'}{\mathrm{d}t} = \boldsymbol{u}(\langle \boldsymbol{X} \rangle + \boldsymbol{X}_d) + X_i' \frac{\partial \boldsymbol{U}(\langle \boldsymbol{X} \rangle + \boldsymbol{X}_d)}{\partial \langle X_i \rangle}. \tag{12}$$

We consider here media that are isotropic at the porescale such that we can write $D_{dij} = D_{dT}\ \delta_{ij} + (D_{dL} - D_{dT}) V_i V_j / V^2$, $D_{dT} = \alpha_{dT} V$, $D_{dL} = \alpha_{dL} V$, where D_{dT}, D_{dL} and α_{dT}, α_{dL} are transverse and longitudinal dispersion coefficients and dispersivities, respectively, and V is the velocity modulus. However, it is consistent with the first-order approximation in σ_Y^2 of (12) to replace $\boldsymbol{V}$ by $\boldsymbol{U}$ in the expression for D_{dij}, i.e. $D_{dij} = \alpha_{dT}\ U \delta_{ij} + (\alpha_{dL} - \alpha_{dT}) U_i U_j / U$ become deterministic and independent of the velocity fluctuations.

Equations (12) permit one to derive the trajectory mean and variances in terms of those of the velocity field (10),(11) and the pore-scale dispersive term $\boldsymbol{X}_d$, and then to determine the spatial moments (7). The main simplification in (12) as compared to (4) is that integration is carried out along the mean advective trajectory, somewhat similar to the 'frozen field' approximation in turbulent transport.

The application of this approach to uniform mean flow is reviewed in § 3, and its extension to radial flow is presented in the remaining sections.

3. Review of transport in mean uniform flow

This case has been investigated in the past. The reason for reviewing it briefly here is to demonstrate that the solution can be simplified considerably for formations of highly anisotropic structures, in order to take advantage of this simplification in solving the transport in radial flow.

3.1. *Solution of the flow and transport problem*

The procedure of § 2.2 simplifies considerably in the case in which the boundary condition is of uniform flow

$$H = -\boldsymbol{J} \cdot \boldsymbol{x} \quad (\boldsymbol{x} \in \partial \boldsymbol{\Omega}), \tag{13}$$

where $\boldsymbol{J}$ is a constant vector. This case has been investigated extensively in the past (see e.g. Dagan 1989). It follows from (8) that $H^{(0)} \equiv -\boldsymbol{J} \cdot \boldsymbol{x}$ and $\boldsymbol{E}^{(0)} \equiv \boldsymbol{J}$ whereas $H^{(1)}$ satisfies the Poisson equation $\nabla^2 H_1 = -\boldsymbol{J} \cdot \nabla Y(\boldsymbol{x})$. As a result, (10), (11) yield at leading order

$$\left.\begin{aligned} \boldsymbol{U} &= K_G \boldsymbol{J}/n, \\ u_{ij}(\boldsymbol{x}' - \boldsymbol{x}'') &= \left(\frac{K_G}{n}\right)^2 [J_i J_j C_Y(\boldsymbol{x}' - \boldsymbol{x}'') + 2J_i C_{E_j Y}(\boldsymbol{x}' - \boldsymbol{x}'') + C_{E_i E_j}(\boldsymbol{x}' - \boldsymbol{x}'')], \end{aligned}\right\} \quad (14)$$

i.e. the velocity field is stationary in an unbounded domain. Finally, from (12) one gets for the trajectories

$$\begin{aligned} \langle \boldsymbol{X} \rangle &= \boldsymbol{a} + \boldsymbol{U}t, \\ X_{ij}(t) &= \langle X_i'(t;\boldsymbol{a}) X_j'(t;\boldsymbol{a}) \rangle \\ &= \int_0^t \int_0^t \langle u_i[\boldsymbol{U}t' + \boldsymbol{X}_d(t')]\, u_j[\boldsymbol{U}t'' + \boldsymbol{X}_d(t'')] \rangle \,\mathrm{d}t'\mathrm{d}t''. \end{aligned} \quad (15)$$

In this case, of mean uniform flow, and under the approximation mentioned above, the pore-scale dispersion tensor has constant components. Without loss of generality we assume the mean flow to be in the x_1-direction and then the covariances of the normal trajectories $\boldsymbol{X}_d$ are given by the simple expressions

$$X_{d11}(t) = 2\alpha_{dL} R, \quad X_{d22}(t) = X_{d33}(t) = 2\alpha_{dT} R, \quad X_{dij} = 0 \ (i \neq j), \quad \text{with} \quad R = Ut. \quad (16)$$

The relationships (15), (16) were employed in order to effectively derive the velocity and trajectory covariances for a few particular, analytical, log-conductivity covariances. Thus, ρ_Y was assumed to be axisymmetric, of the form $\rho_Y(\boldsymbol{x}) = \rho_Y[(x_1^2 + x_2^2)/I^2, x_3^2/I_v^2]$ (Gelhar & Axness 1983), where x_3 is a vertical coordinate. In particular, the two common expressions adopted in the past were the exponential and Gaussian ones

$$\rho_Y(\boldsymbol{x}) = \exp\{-[(x_1^2 + x_2^2)^2/I^2 + x_3^2/I_v^2]^{1/2}\}, \quad \rho_Y(\boldsymbol{x}) = \exp[-\pi(x_1^2 + x_2^2)^2/4I^2 - \pi x_3^2/4I_v^2], \quad (17)$$

where I and I_v are the horizontal and vertical linear integrals scales, respectively, defined by $I = \int_0^\infty \rho_Y(x_1, 0, 0)\,\mathrm{d}x_1$ and $I_v = \int_0^\infty \rho_Y(0, 0, x_3)\,\mathrm{d}x_3$. Under these simple representations the various flow variables depend on the parameters K_G, σ_Y^2, I, $e = I_v/I$, $Pe = UI/D_{dT} = I/\alpha_{dT}$ and α_{dT}/α_{dL}. For sedimentary formations, the anisotropy ratio e is as a rule smaller than unity. We restrict our work to the results pertinent to the longitudinal $X_{11}(t)$ solely.

The computation of $X_{11}(t)$ can be carried out conveniently with the aid of the Fourier transform of the velocity covariance in (15) and the general expression for X_{ij} is given in terms of a few quadratures (e.g. Dagan 1987). Similar expressions were obtained from a first-order approximation of the Eulerian transport equation by Naff (1990). In both cases of ρ_Y (17), and in fact for any ρ_Y of finite integral scales and of arbitrary e, the asymptotic limit of X_{11} for $R/I = Ut/I \gg 1$ is given by $X_{11} \to 2\alpha_{11} Ut$, where $\alpha_{11} = D_{11}/U$ is the longitudinal 'macrodispersivity' depending generally on Pe, e and the ratio α_{dT}/α_{dL}. Fiori (1996) has computed effectively $X_{11}(t; e, Pe)$ for the exponential ρ_Y (17) and presented graphs of the asymptotic α_{11} (18) as function of Pe, for different $e < 1$. A property of α_{11} that is of relevance for the present study, following from Fiori (1996, figure 1), is that the longitudinal pore-scale dispersion has a negligible effect upon α_{11} for $Pe > 1$. Since in the applications considered here we are interested in transport of large $Pe = I/\alpha_{dT}$, we take $\alpha_{dL} = 0$ and this approximation

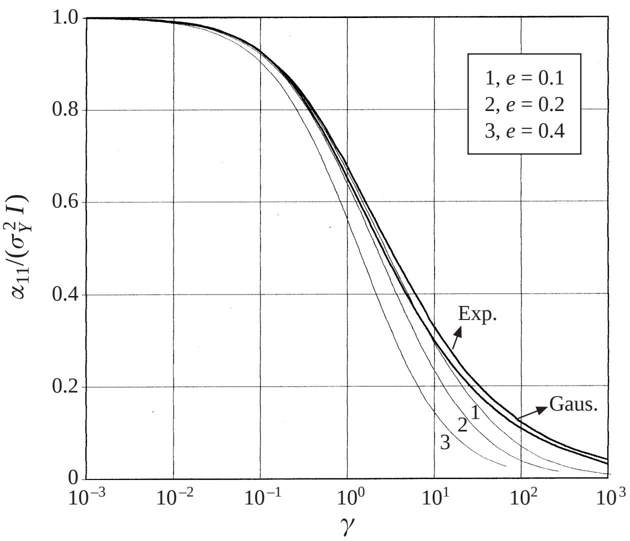

FIGURE 1. Asymptotic longitudinal macrodispersivity α_{11} for mean uniform flow as function of $\gamma = (e^2 Pe)^{-1}$ for a few values of the anisotropy ratio e. (Thin line complete solution by Fiori, 1996; thick lines, approximation (20) for exponential and Gaussian covariances.)

becomes even more accurate for $e < 1$. In other words, the mixing effect of pore-scale dispersion upon longitudinal trajectory fluctuations is manifested mainly through transfer of solute across streamtubes. With this assumption the large-time (large travel distance) limit of the trajectory variance is given by

$$X_{11} \to 2\,\alpha_{11} U t, \quad \alpha_{11} = \sigma_Y^2\, I\, f_L(e, Pe) \quad (Ut/I \gg 1). \tag{18}$$

In the case of infinite Pe, i.e. with neglect of pore-scale dispersion, $\alpha_{11} = \sigma_Y^2 I$ and $f_L = 1$ are independent of e altogether.

Another major simplification of α_{11} can be achieved for anisotropic formations of $e \ll 1$. Thus, simplified relationships were obtained for the exponential ρ_Y (17) by Gelhar & Axness (1983) and Naff (1990), by an expansion of the complete expression for α_{11} in a power series in e and retaining the leading-order term. However, they do not compare the result of this approximation with the complete first-order approximation, valid for any e and Pe or for ρ_Y other than the exponential. A close examination of the expression for α_{11} shows that this small e approximation is obtained for any ρ_Y by retaining the first term of u_1 in (10), and the vertical pore-scale dispersion component only in (15), i.e.

$$u_1(\boldsymbol{x}) = U\, Y'(\boldsymbol{x});$$
$$X_1'(t) = \int_0^t u_1[Ut', 0, X_{d3}(t')]\, \mathrm{d}t' = \frac{U}{(2\pi)^{3/2}} \int_0^t \int \widehat{Y}'(\boldsymbol{k})\, \mathrm{e}^{-\mathrm{i}k_1 Ut' - \mathrm{i}k_3 X_{dT}(t')}\, \mathrm{d}\boldsymbol{k}\, \mathrm{d}t' \tag{19}$$

$$\left.\begin{aligned} X_L(t) &= \langle [X_1'(t)]^2 \rangle = \frac{U^2 \sigma_Y^2}{(2\pi)^{3/2}} \int_0^t \int_0^t \int \widehat{\rho}_Y(\boldsymbol{k})\, \mathrm{e}^{-\mathrm{i}k_1 U(t'-t'')} \mathrm{e}^{-k_3^2 a_{dT} U|t'-t''|} \mathrm{d}\boldsymbol{k}\, \mathrm{d}t'\, \mathrm{d}t'', \\ \alpha_L &= \frac{1}{2U} \frac{\mathrm{d}X_L}{\mathrm{d}t} = \frac{U\sigma_Y^2}{(2\pi)^{3/2}} \int_0^t \int \widehat{\rho}_Y(\boldsymbol{k}) \cos(k_1 U t') \mathrm{e}^{-k_3^2 a_{dT} U t'} \mathrm{d}\boldsymbol{k}\, \mathrm{d}t'. \end{aligned}\right\} \tag{20}$$

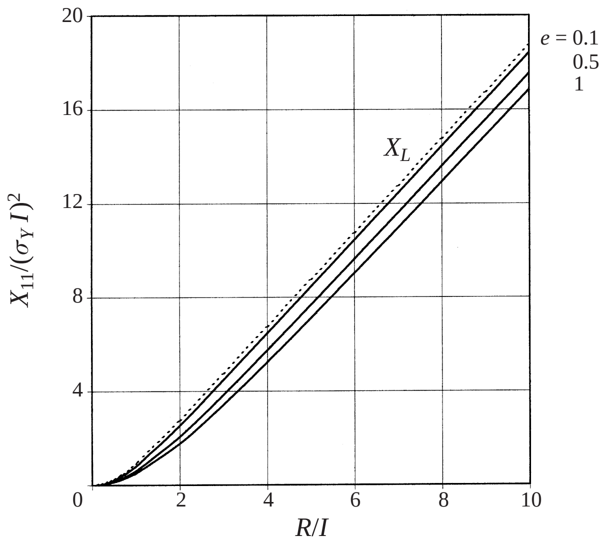

FIGURE 2. Trajectory variance X_{11} for mean uniform flow as function of travel distance $R/I = Ut/I$ for a few values of the anisotropic ratio e, Gaussian ρ_Y and infinite Pe. (Full lines, complete solution; dotted line, approximation X_L (20).)

In (19) Y' is the log-conductivity fluctuation and the Fourier transform is defined by $\widehat{f}(\boldsymbol{k}) = (2\pi)^{-3/2} \int f(\boldsymbol{x}) \exp(\mathrm{i}\boldsymbol{k} \cdot \boldsymbol{x})\,\mathrm{d}\boldsymbol{x}$, and advantage was taken of the stationarity of Y. The notation $\boldsymbol{X}_L$ and α_L stands for X_{11} and α_{11} under the approximation (19).

While the complete solutions of $\boldsymbol{X}_{11}$ and α_{11} depend on $Pe = I/\alpha_{dT}$ and $e = I_v/I$, it was observed by Gelhar & Axness (1983) and Naff (1990) that the simplified solution X_L, α_L depends on the unique parameter $\gamma = (e^2 Pe)^{-1} = \alpha_{dT} I/I_v^2$.

To assess the accuracy of this approximation, which is crucial for simplifying the solution of transport in radial flow, we compare in figure 1 the complete large-time asymptotic solution $\alpha_{11}(Pe, e)$ (18), (14), (15) derived by Fiori (1996, figure 1) for the exponential ρ_Y and $\alpha_L(\gamma)$ of (20). It is emphasized that for applications of interest in contaminant transport through aquifers, generally $\gamma < 1$.

Examination of figure 1 shows that α_L (20) is an accurate approximation of α_{11} for $e < 0.2$ and for $\gamma < 1$. For infinite Pe, more precisely for $\gamma < 0.01$, α_{11} is independent of e and it reaches the value $\alpha_{11} = \alpha_L = \sigma_Y^2 I$ (e.g. Gelhar & Axness 1983). It is also seen from figure 1 that the asymptotic α_L for the two ρ_Y (the exponential and the Gaussian, (17)), differ very little.

As a matter of fact, the approximation (20) simplifies the computation of $X_L(t)$ and of $\alpha_L(t) = (1/U)\,\mathrm{d}X_L/\mathrm{d}t$ for any t. In figure 2 we compare the approximate $X_L(R)$ (20) with the trajectory longitudinal variance derived by the complete expression for infinite Pe (see figure 4.6.1 of Dagan 1989 and the analytical result for isotropic media in Dagan 1984). It is seen that (20) provides an accurate result in this case at any $R = Ut$, and not only for large R/I (figure 1).

Finally, Monte Carlo numerical simulations of two-dimensional flow (Bellin, Salandin & Rinaldo 1992) and the recent ones of three-dimensional flow (Chin 1997) have demonstrated that the first-order approximation of X_{11} is accurate for σ_Y as large as 1.5. It seems that this unexpected robustness stems from mutual cancellation of the flow and trajectory higher-order terms.

3.2. *Spatial moments of a solute plume*

The case mostly analysed in the past was of a plume of constant initial concentration C_0 injected instantaneous in a finite volume V_0. Without loss of generality we shall consider an area A_0 in the vertical plane $x_1 = 0$ and a thin initial plume, of infinitesimal thickness Δa_1 normal to A_0. With $\rho_0 = nC_0\Delta a_1$, the density of solute per unit injection area, the concentration (5) now becomes $C = \rho_0 \int_{A_0} \delta[\boldsymbol{x} - \boldsymbol{X}_t(t;\boldsymbol{a})]\,\mathrm{d}\boldsymbol{a}$ and the spatial moments (7) are given by the simple relationships

$$M = \rho_0 A_0, \quad R_1 = \langle X_1(t;0,a_2,a_3)\rangle = Ut, \quad S_{11} = X_{11}(t;Pe,e), \tag{21}$$

where we have neglected the additional term $X_{d11} = 2\alpha_{dL}Ut$ of S_{11} by virtue of $Pe \gg 1$.

More recently Cvetkovic & Dagan (1994) have discussed the case of continuous injection in time at constant C_0 over the area A_0. Assuming that injection takes place during an infinitesimal time Δt, the solution for $C(5)$ is still valid if the volume V_0 is defined by A_0 and by the variable and random dimension $\Delta a_1 = V_1(0,a_2,a_3)\,\Delta t$ normal to A_0. With the average density given by $\rho_0 = nC_0U\Delta t$, the impact of the exact random initial condition upon R_1 and S_{11} was found to be small (of higher order in σ_Y^2 than the first) and furthermore, the additional terms in (21) decay quickly with the distance from the injection plane. Hence, the moments (21) are valid for both modes of injection, instantaneous or continuous.

Summarizing this section, we have demonstrated that the simplified solution of the spatial longitudinal moments, suggested by Gelhar & Axness (1983) and Naff (1990), can be obtained from the approximate expressions of the velocity and trajectory (19). Furthermore, we have shown that it leads to accurate asymptotic values of the macro-dispersivity for finite Pe and for anisotropic formations of, say, $e < 0.2$ and for the trajectory variance at any time for infinite Pe. These results are instrumental in simplifying the problem of transport in radial flow.

4. Transport in radial flow

4.1. *Solution of the flow problem*

We consider flow from a fully penetrating well of radius r_w through a formation of thickness $2L_3$. With x_3 along the well axis, the planes $x_3 = \pm L_3$ are assumed to be impervious, and the flow is driven by the difference between the constant head H_w on the well surface $A_0 = 4\pi r_w L_3$ and the constant H_L on an exterior boundary $r = L$. Here, $r = (x_1^2 + x_2^2)^{1/2}$ and $\theta = \tan^{-1}(x_2/x_1)$ are radial coordinates in the horizontal plane. Our aim is to derive the velocity covariances in the domain $\boldsymbol{\Omega}$ defined by $r_w \leqslant r \leqslant L$, $|x_3| \leqslant L_3$ for an anisotropic axisymmetric structure of ρ_Y (17).

This problem has been investigated by Indelman *et al.* (1996) and Fiori *et al.* (1998) toward determining the equivalent conductivity, which is defined as that of a fictitious homogeneous formation that conveys the same total discharge per unit length Q as the actual one. We adopt the same simplifying assumptions:

(i) We solve at first order in σ_Y^2 for the reasons discussed in the previous Sections. Thus, the general equations (8)–(11) constitute our starting point.

(ii) The thickness $L_3 \to \infty$. This assumption is justified if $L_3/I_v \gg 1$, which is a condition met in most applications. The solution is affected only in the neighbourhood of the upper and lower boundaries. By the same token, this assumption ensures ergodicity in the sense that ensemble averaging can be exchanged with space averaging along vertical lines.

(iii) We let $r_w \to 0$ and replace the well by a singular line, which is justified if $r_w/I \ll 1$, a condition which is again satisfied in most applications. The study of Indelman *et al.* (1996) indicates that this is a valid approximation for $r_w/I < 0.2$.

(iv) The formation is assumed to be unbounded in the horizontal plane, i.e. $L \to \infty$, which implies $L/I \gg 1$. In the process of taking the last two limits the discharge Q, which is proportional to $(H_w - H_L)/\ln(L/r_w)$, is kept constant and the constant boundary heads become immaterial as far as the velocity field is concerned.

Under these conditions the mean velocity is given by

$$\langle V_r \rangle = U = \frac{Q}{2\pi n r}, \quad \langle V_\theta \rangle = \langle V_3 \rangle = 0, \tag{22}$$

while in (8) $H^{(0)}(r)$ satisfies $\nabla^2 H^{(0)} = -(Q/K_G)\,\delta(r)$. Thus, the zero-order term of the head gradient $\boldsymbol{E}$ is given by

$$E_r^{(0)} = \frac{Q}{2\pi K_G r}, \quad E_\theta^{(0)} = E_3^{(0)} = 0. \tag{23}$$

In the same vein, $H^{(1)}$ (8) satisfies $\nabla^2 H^{(1)} = E_r^{(0)}\,\partial Y'/\partial r$. Since we are concerned here with radial dispersion, we need to evaluate the velocity covariance along radii (see §4.2) $u_{rr}(r', r'') = \langle u_r(r', \theta, x_3)\, u_r(r'', \theta, x_3) \rangle$. By substituting this in (11) we obtain

$$u_{rr}(r', r'') = \left(K_G/n\right)^2 [C_Y(r' - r'')E_r^{(0)}(r')E_r^{(0)}(r'') + C_{E_rY}(r'', r')E_r^{(0)}(r') + C_{E_rY}(r', r'')E_r^{(0)}(r'') + C_{E_rE_r}(r', r'')] \tag{24}$$

where C_Y, C_{E_rY} and $C_{E_rE_r}$ are two-point covariances of Y and $E_r^{(1)}$ at r', θ, x_3 and r'', θ, x_3, respectively. Owing to the axisymmetry of the mean flow, all these covariances are independent of θ and x_3, but they are not stationary in r' and r''.

The main difficulty in evaluating u_{rr} stems from the covariances in the last three terms of (24) (Fiori *et al.* 1998). Their detailed expressions and their impact upon transport are examined in Appendix A. In line with the approximation adopted for uniform flow (figures 1 and 2) for sufficiently small e, we shall develop a similar simplified solution for radial flow.

4.2. *Solution of the transport problem*

We consider a plume of constant C_0, injected through the well envelope A_0 during an infinitesimal time Δt. Similarly to the uniform flow case, the spatial moments can be determined accurately for the equivalent case of an initial thin plume of radial constant dimension $\Delta r_0 = nU(r_w)\,\Delta t$ surrounding the well (figure 3). With $\rho_0 = C_0 \Delta r_0$, the concentration field (5) is given by

$$C(\boldsymbol{x}, t) = \rho_0 \int_{A_0} \delta[\boldsymbol{x} - \boldsymbol{X}_t(t; \boldsymbol{a})]\, \mathrm{d}\boldsymbol{a} \tag{25}$$

while the plume mass is $M = \rho_0 A_0$.

At time t the plume is advected outwards and is distorted due to heterogeneity (figure 3). In analogy with the centroid of a plume in a mean uniform flow, we define a front by $R = (1/M) \int rC\mathrm{d}\boldsymbol{x}$ (figure 3). In a homogeneous medium R is the location of the thin plume at time t. Assuming ergodic conditions we get from (25) $R(t) = \langle R \rangle = \langle X_r \rangle$. From (12), (22) we obtain

$$\frac{\mathrm{d}\langle X_r \rangle}{\mathrm{d}t} = \frac{Q}{2\pi n \langle X_r \rangle}, \quad \text{i.e.} \quad R = \langle X_r \rangle = \left(\frac{Qt}{\pi n}\right)^{1/2}, \tag{26}$$

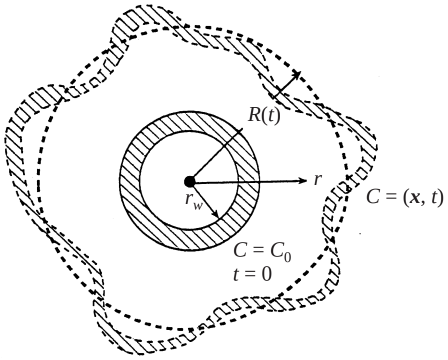

FIGURE 3. Definition sketch for solute spreading by radial divergent flow (horizontal cross-section).

where we have taken $R(0)$ equal to zero rather than r_w, consistent with our approximation of the well boundary condition. In a similar vein, the rate of spreading of the plume around the front is characterized by $S_{rr}(t) = (1/M)\int (r-R)^2 C \mathrm{d}\boldsymbol{x}$ leading by (25) to $S_{rr}(t) = \langle S_{rr}\rangle = X_{rr} + X_{drr}$. It is emphasized that the effect of spreading represented by $X_{rr} = \langle X_r'^2(t)\rangle$ is due entirely to the heterogeneous structure and it vanishes for $\sigma_Y^2 = 0$. In contrast, a finite plume undergoes an additional stretching that occurs in a homogeneous medium as well due to the mean flow non-uniformity (this effect is examined in Appendix B). For the high Pe of interest here, X_{drr} is small in comparison with X_{rr} and is neglected hereafter.

The trajectory fluctuation is derived at first order from the general equation (12), which now becomes

$$\frac{\mathrm{d}X_r'}{\mathrm{d}t} = u_r(R, 0, X_{d3}) + X_r'\frac{\mathrm{d}U}{\mathrm{d}R}. \tag{27}$$

Since we limit the derivations to anisotropic formations of, say, $e < 0.2$, and in line with the findings regarding mean uniform flow, we have maintained in (27) the effect of transverse pore-scale dispersion in the vertical direction only. The variance of X_{d3} is evaluated approximately, consistent with other approximations adopted here, by regarding it as attached to the time-dependent mean flow at the front, i.e.

$$X_{d33} = \langle X_{d3}^2(t)\rangle = 2\alpha_{dT}\int_0^t U(t')\,\mathrm{d}t' = 2\alpha_{dT}R. \tag{28}$$

Switching to R (26) rather than t as independent variable and integrating in (27) with $X_r' = 0$ for $R = 0$, yields the basic result

$$\left.\begin{aligned} X_r'(R) &= U(R)\int_0^R \frac{u_r(r, 0, X_{d3})}{U^2(r)}\mathrm{d}r, \\ X_{rr}(R) = \langle X_r'^2(R)\rangle &= U^2(R)\int_0^R\int_0^R \frac{u_{rr}(r', 0, X_{d3}(r'), r'', 0, X_{d3}(r''))}{U^2(r')U^2(r'')}\mathrm{d}r'\mathrm{d}r''. \end{aligned}\right\} \tag{29}$$

We are now in a position to characterize transport by spatial moments in radial flow for any given ρ_Y by deriving first the covariances $C_{E_rY}(r', r'')$ and $C_{E_rE_r}(r', r'')$, then the velocity autocorrelation (24) and finally X_{rr} (29). This is still a difficult task because of the large number of quadratures involved and we shall further simplify the procedure.

First, in order to illustrate the results, we have computed the expressions for C_{E_rY} and $C_{E_rE_r}$ appearing in (24) that are written explicitly in Appendix A (A 4), (A 5)

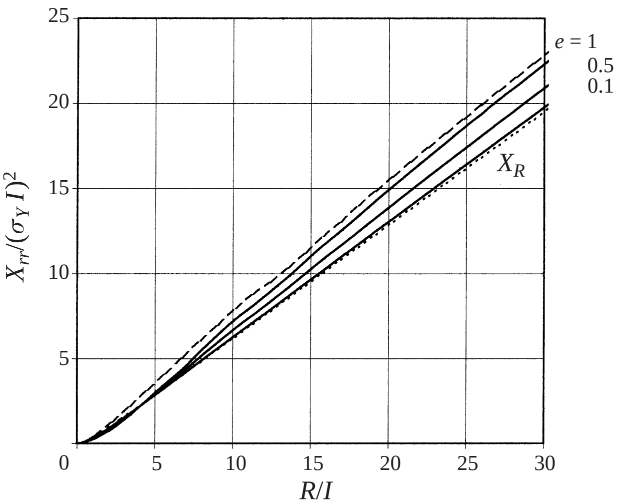

FIGURE 4. Trajectory variance X_{rr} for mean radial flow as function of travel distance of the mean front for Gaussian correlation and infinite Pe. Full lines, complete solution (43), (A 9), (A 10) for small e; dotted line, approximation X_R (43); dashed line, complete solution for isotropic media (43), (A 6), (A 7).

for a Gaussian ρ_Y (17). Subsequently, we split, for convenience of notation, X_{rr} (29) into the three terms stemming from the corresponding three terms of u_{rr} (24), i.e. $X_{rr} = X_R + X_{rr}^{EY} + X_{rr}^{EE}$. The first contribution, X_R, is similar to X_L (19) for uniform flow. Hence, by using the approximation $u_{rr}(\boldsymbol{x}', \boldsymbol{x}'') \simeq (K_G/n)^2 C_Y(r' - r'') E_r^{(0)}(r') E_r^{(0)}(r'') = \sigma_Y^2 \rho_Y(\boldsymbol{x}' - \boldsymbol{x}'') U(r') U(r'')$, X_R can be written with the aid of (29) as

$$X_R(R) = \sigma_Y^2 U^2(R) \int_0^R \int_0^R \langle \rho_Y [r' - r'', 0, X_{d3}(r') - X_{d3}(r'')] \rangle \frac{\mathrm{d}r' \mathrm{d}r''}{U(r')U(r'')}, \qquad (30)$$

where averaging here is over the pore-scale dispersion random fluctuations X_{d3}.

The results obtained for uniform flow (figure 2) suggest that X_R (30) may be an accurate approximation of X_{rr} (29) for sufficiently small e. We have checked in part this assumption by carrying out in Appendix A the computation of the full expression for $X_{rr}(R)$ (29) for infinite Pe and for the Gaussian ρ_Y and the result (30), (A 6) is compared with X_R (dotted line) in figure 4. The dashed line in figure 4 represents the complete expression for X_{rr} for isotropic formation (requiring 6 quadratures), whereas the continuous curves are valid for small anisotropy ratio e (expressions (30), (A 9)) and imply 5 quadratures (Fiori *et al.* 1998). It is seen that for small e the approximation X_R is very close to X_{rr}.

Relying on these sets of results (figures 1, 2 and 4) we proceed with the analysis of transport in radial flow based on the approximation (30).

4.3. *Analysis of transport for* $X_{rr} \approx X_R$

Applying the Fourier transform to (30) we get

$$X_R(R) = \frac{\sigma_Y^2 U^2(R)}{(2\pi)^2} \int_0^R \int_0^R \frac{1}{U(r')U(r'')} \iiint \widehat{\rho}_Y(\mathbf{k}) \times \exp[-\mathrm{i}k_1(r' - r'')] \; \langle \exp\{-\mathrm{i}k_3[X_{d3}(r') - X_{d3}(r'')]\} \rangle \; \mathrm{d}\boldsymbol{k} \, \mathrm{d}r' \, \mathrm{d}r''. \qquad (31)$$

Averaging over the pore-scale dispersion component X_{d3} leads to

$$\langle \exp\{-\mathrm{i}k_3[X_{d3}(r') - X_{d3}(r'')]\}\rangle = \exp(-k_3^2 \alpha_{dT} |r' - r''|). \tag{32}$$

Substitution of (32) in (31) and using the definitions of $U(r)$ (22) and $R(t)$ (26) yields the general relationship

$$X_R(R) = \frac{\sigma_Y^2}{(2\pi)^{3/2}R^2} \int_0^R \int_0^R \iiint \widehat{\rho}_Y(\boldsymbol{k}) \exp[-\mathrm{i}k_1(r' - r'') - k_3^2\alpha_{dT} |r' - r''|]\, r' r'' \, \mathrm{d}\boldsymbol{k}\, \mathrm{d}r' \, \mathrm{d}r''. \tag{33}$$

Equation (33) is the counterpart of X_L (19) for uniform flow. We illustrate the results for the exponential and Gaussian ρ_Y separately.

(i) *Exponential log-conductivity covariance* (17)

The Fourier transform of ρ_Y is given by

$$\widehat{\rho}_Y(\boldsymbol{k}) = \frac{2^{3/2} I^2 I_v}{\pi^{1/2}(1 + k_1^2 I^2 + k_2^2 I^2 + k_3^2 I_v^2)^2}. \tag{34}$$

Substituting in (33), integrating over k_2 and r' and switching to the variables $p_1 = k_1 I$, $p_3 = k_3 I_v$, $\overline{R} = R/I$ leads to

$$\frac{X_R}{I^2} = \frac{\sigma_Y^2}{6\pi \overline{R}^2} \int_0^{\overline{R}} \int_{-\infty}^{\infty} \int_{-\infty}^{\infty} \frac{(\overline{R} - r)^2 (2\overline{R} + r)}{(1 + p_1^2 + p_3^2)^{3/2}} \cos(p_1 r) \exp(-\gamma p_3^2)\, r \, \mathrm{d}p_1 \mathrm{d}p_3 \, \mathrm{d}r, \tag{35}$$

where $\gamma = \alpha_{dT} I / I_v^2 = (e^2 Pe)^{-1}$ was defined before, in the discussion of transport in mean uniform flow. Equation (35) can be used in order to evaluate $X_R/(\sigma_Y^2 I^2)$ as function of $\overline{R}$ and γ. This will be done effectively for the Gaussian covariance below, while for the exponential one we derive the asymptotic 'macrodispersion' coefficients in § 4.4.

(ii) *Gaussian log-conductivity covariance* (17)

For convenience, we can rewrite (17) as $\rho_Y(\boldsymbol{x}) = \rho_Y(r)\rho_Y(x_3) = \exp[-\pi\left(r/2I\right)^2]\exp[-\pi\left(x_3/2I_v\right)^2]$.

With $\widehat{\rho}_Y(k_3) = \sqrt{2} I_v/\pi^{1/2} \exp(-k_3^2 I_v^2/\pi)$, substitution in (33) yields

$$\begin{aligned} X_R(R) &= \frac{\sigma_Y^2}{(2\pi)^{1/2}R^2} \int_0^R \int_0^R r' r'' \rho_Y(r' - r'') \int_{-\infty}^{\infty} \widehat{\rho}_Y(k_3) \exp(-k_3^2 \alpha_{dT} |r' - r''|)\, \mathrm{d}k_3 \, \mathrm{d}r' \, \mathrm{d}r'' \\ &= \frac{\sigma_Y^2}{R^2} \int_0^R \int_0^R \frac{r' r'' \rho_Y(r' - r'')}{(1 + \pi \alpha_{dT} I_v^{-2} |r' - r''|)^{1/2}} \mathrm{d}r' \mathrm{d}r'' \\ &= \frac{\sigma_Y^2 I^2}{3\overline{R}^2} \int_0^{\overline{R}} \frac{(\overline{R} - r)^2 (2\overline{R} + r)}{(1 + \pi\gamma r)^{1/2}} \exp(-\pi r^2/4) \mathrm{d}r. \end{aligned} \tag{36}$$

We have represented $X_R/(\sigma_Y^2 I^2)$ (36) as a function of $\overline{R} = R/I$ for a few values of $\gamma = (e^2 Pe)^{-1}$ in figure 5 and for comparison $X_L/(\sigma_Y^2 I^2)$ (20) for $\gamma = 0$. It is seen that the spreading due to heterogeneity is much smaller in radial flow than in a uniform one, for the same distance from the source.

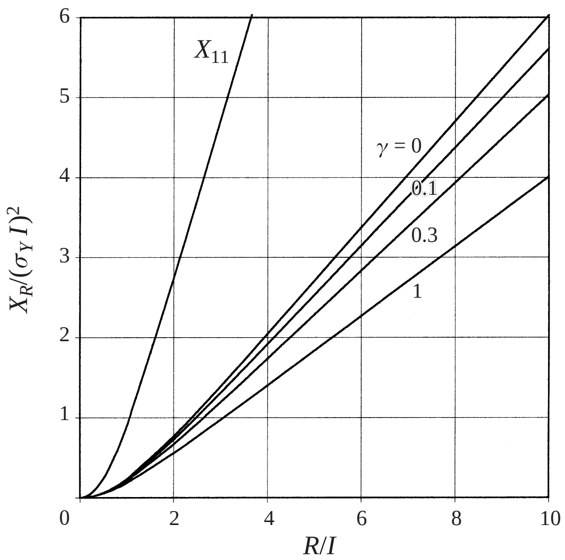

FIGURE 5. Trajectory variance X_R (36) for radial flow as function of mean front location $R = Ut$ for a few values of γ and for Gaussian correlation function (X_{11} is the longitudinal trajectory variance for mean uniform flow).

4.4. *Apparent and equivalent 'macrodispersivities'*

The mean displacement R and its variance X_R define the motion of an ergodic plume and its spreading in terms of centroid location and the second spatial moment. However, to derive the expression for the mean concentration $\langle C(\boldsymbol{x}, t)\rangle$ with the aid of (5) one needs the entire p.d.f. $f(X_R)$ of X_R, and not just its mean and variance. Under the first-order approximation (27) adopted here X_R is normal, since it results from a linear operator applied to Y. Furthermore, X_R tends to normality asymptotically under general conditions, for $\overline{R} \gg 1$, by virtue of the central limit theorem. Although $f(X_R)$ has a simple analytical expression, it is of interest, for the purpose of comparison with transport in homogeneous formations, to write the Focker–Planck equation satisfied by $\langle C\rangle$

$$\frac{\partial\langle C\rangle}{\partial t} + U(t)\,\frac{\partial\langle C\rangle}{\partial r} = D_R^{(app)}(t)\,\frac{\partial^2\langle C\rangle}{\partial r^2} \quad U = \frac{\mathrm{d}R}{\mathrm{d}t} \quad D_R^{(app)}(t) = \frac{1}{2}\,\frac{\mathrm{d}X_R}{\mathrm{d}t}, \tag{37}$$

where $D_R^{(app)}$ is defined as the apparent macrodispersion coefficient. The reason to adopt this definition is that (37) can be viewed as describing transport in a mean uniform velocity field $U(t)$ and with macrodispersion coefficient $D_R^{(app)}(t)$. It is emphasized that $D_R^{(app)}(t)$ is non-local in the sense that t stands for the travel time of a marked fluid particle by the mean velocity field. Asymptotically, for $R/I \gg 1$, one can define an asymptotic constant apparent macrodispersivity $\alpha_R^{(app)} = D_R^{(app)}/U$. This leads for the exponential covariance (17), after a quadrature in (35) and for $\overline{R} \to \infty$, to

$$\frac{\alpha_R^{(app)}(\gamma)}{I} = \frac{\sigma_Y^2}{6\pi}\int_{-\infty}^{\infty}\int_{-\infty}^{\infty}\frac{\gamma p_3^2}{(p_1^2+\gamma^2 p_3^4)(1+p_1^2+p_3^2)^{3/2}}\mathrm{d}p_1\mathrm{d}p_3. \tag{38}$$

This result is identical to that of Naff (1990) for uniform flow (after one integration) except for a factor of 1/3 in (38).

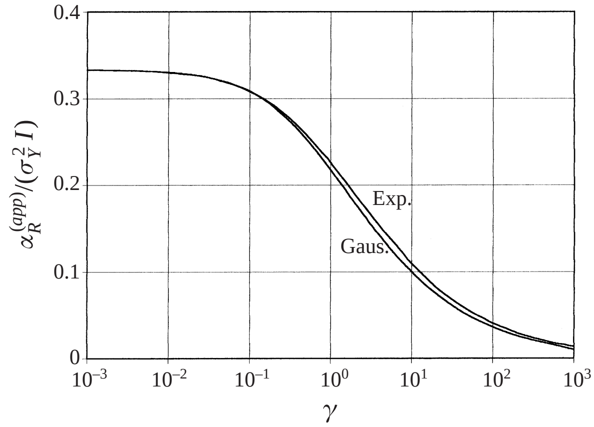

FIGURE 6. Asymptotic apparent macrodispersivity $\alpha_R^{(app)}$ for radial flow as function of $\gamma = (e^2 Pe)^{-1}$ for exponential (39) and Gaussian (40) correlations.

Switching to polar coordinates in (38) and integrating over the radial variable yields

$$\frac{\alpha_R^{(app)}(\gamma)}{I} = \frac{4\sigma_Y^2}{3\pi} \int_0^{\pi/2} \frac{\Theta}{1-\Theta^2} \left[1 - \frac{\Theta\, S(\Theta)}{(1-\Theta^2)^{1/2}}\right] \frac{\mathrm{d}\phi}{\cos\phi} \tag{39}$$

where

$$S(\Theta) = \begin{cases} \operatorname{arccotan} \dfrac{\Theta}{(1-\Theta^2)^{1/2}} & \text{for } \Theta < 1 \\ \frac{1}{2}\ln \dfrac{\Theta + (\Theta^2-1)^{1/2}}{\Theta - (\Theta^2-1)^{1/2}} & \text{for } \Theta > 1, \end{cases} \qquad \Theta(\phi) = \gamma \frac{\sin^2\phi}{\cos\phi}.$$

We have plotted $\alpha_R^{(app)}/(\sigma_Y^2 I)$ (39) as function of γ in figure 6. The striking result is that $\alpha_R^{(app)}$ is much smaller than α_L (figure 1) for uniform flow, by a factor of 3. In particular, for $Pe \gg 1$, i.e. for $\gamma \ll 1$, we get in (39) the simple result $\alpha_R^{(app)}(0)/(\sigma_Y^2 I) = 1/3$ as compared with $\alpha_L(0)/(\sigma_Y^2 I) = 1$.

In the same vein, the asymptotic apparent macrodispersivity for the Gaussian ρ_Y (17) is obtained from (36) as

$$\frac{\alpha_R^{(app)}(\gamma)}{I} = \frac{\sigma_Y^2}{3} \int_0^{\infty} \frac{\exp(-\pi r^2/4)}{(1+\pi\gamma r)^{1/2}} \mathrm{d}r. \tag{40}$$

Again, we have represented $\alpha_R^{(app)}/(\sigma_Y^2 I)$ (40) as function of $\overline{R}$ in figure 6 and the result is indistinguishable from the one pertaining to the exponential covariance (39). It is seen that for small γ we again get $\alpha_R^{(app)}/(\sigma_Y^2 I) = 1/3$. In the context of field experiments $\alpha_R^{(app)}$ can be viewed as resulting from the interpretation of a breakthrough or of spatial mapping of a plume at a time t in which the interpreter assumes that flow is uniform.

A related, but different coefficient, which we call equivalent macrodispersivity, is defined as the one pertaining to transport in radial flow in a homogeneous formation, such that the centroid velocity $\mathrm{d}R/\mathrm{d}t$ and the rate of change of the second spatial moment of the plume $\frac{1}{2}\,\mathrm{d}S_{rr}/\mathrm{d}t$ are equal to those prevailing in the heterogeneous formation. In mathematical terms we seek the solution of

$$\frac{\partial\langle C\rangle}{\partial t}+V(r)\frac{\partial\langle C\rangle}{\partial r}=\frac{1}{r}\frac{\partial}{\partial r}\left[\alpha_R^{(eq)}rV(r)\,\frac{\partial\langle C\rangle}{\partial r}\right],\quad V=\frac{Q}{2\pi r}, \tag{41}$$

for the initial condition of a pulse, such that $\langle C\rangle$ has first and second spatial moments rates of change equal to U (22) and $\mathrm{d}X_R/\mathrm{d}t$ (33), respectively. Unlike mean uniform flow, it is generally not possible to derive values of Q and $\alpha_R^{(eq)}(t)$ to satisfy these requirements. This is possible, however, for large $\overline{R}$ if we adopt the approximate, boundary layer, solution of (41) derived by Gelhar & Collins (1971). Indeed, by the nature of this approximation and for the given Q, the velocity of the plume centroid is equal to U (22). Furthermore, their equation (32) leads to the rate of change of the second spatial moment $\frac{1}{2}\,\mathrm{d}S_{rr}/\mathrm{d}t=\alpha_R^{(eq)}/3$. The same result is obtained after some manipulations from the boundary layer solution of (41) of Dagan (1971).

By comparing the latter result with the asymptotic one in the heterogeneous formation (39), (40) we arrive at the simple result that $\alpha_R^{(eq)}=\alpha_L$, i.e. the asymptotic equivalent macrodispersivity is equal to the one prevailing in uniform flow. In particular, for infinite Pe, $\alpha_R^{(eq)}=\sigma_Y^2 I$. This result is in agreement with the similar one in Indelman *et al.* (1996) for the equivalent conductivity in radial flow that tends to the effective one in mean uniform flow far from the well.

Thus, $\alpha_R^{(eq)}$ can be viewed as the value of the longitudinal dispersivity to be adopted in a code that solves the problem of radial transport in a homogeneous formation, to represent the effect of heterogeneity at a large distance from the well.

4.5. *Analysis of transport for* $Pe\to\infty$

It is seen in figure 6 that for $\gamma<0.01$ one can neglect the transverse mixing ($Pe=\infty$). This constitutes a classic topic of pure advective transport of an inert tracer. By taking $\alpha_{dT}=0$ in (30) we can express X_R in terms of a single quadrature as

$$X_R(R)=\frac{2\sigma_Y^2 R}{3}\int_0^R\left(1-\frac{3r}{2R}+\frac{r^3}{2R^3}\right)\rho_Y^h(r)\,\mathrm{d}r \tag{42}$$

to be compared with $X_L=2\sigma_Y^2 L\int_0^L(1-x/L)\,\rho_Y(x)\,\mathrm{d}x$ for uniform flow.

One can easily calculate the trajectory variance (42) in particular cases. Thus

$$\frac{X_R}{I^2\sigma_Y^2}=\frac{2\overline{R}}{3}\left[\mathrm{erf}\left((\pi\overline{R})^{1/2}/2\right)+\frac{4-3\pi\overline{R}^2+2(\pi\overline{R}^2-2)\exp\left(-\pi\overline{R}^2/4\right)}{\pi^2\overline{R}^3}\right] \tag{43}$$

for the Gaussian ρ_Y and

$$\frac{X_R}{I^2\sigma_Y^2}=\frac{2\overline{R}}{3}-1-\frac{2}{\overline{R}^2}\left[(1+\overline{R})\exp\left(-\overline{R}\right)-1\right] \tag{44}$$

for the exponential covariance function, with $\overline{R}=R/I$. These two results are compared with the corresponding ones for uniform flow in figure 7. As we have mentioned before for finite Pe, the asymptotic longitudinal apparent macrodispersivity is obtained as

$$\alpha_R^{(app)}=\lim_{R\to\infty}\frac{1}{2}\frac{\mathrm{d}X_R(R)}{\mathrm{d}R}=\lim_{R\to\infty}\frac{\sigma_Y^2}{3}\int_0^R\left(1-\frac{r^3}{R^3}\right)\rho_Y^h(r)\,\mathrm{d}r=\frac{\sigma_Y^2 I}{3}=\frac{\alpha_L}{3}. \tag{45}$$

It is seen that for any ρ_Y of finite horizontal integral scale we get in (45) $\alpha_R^{(app)}\to\sigma_Y^2 I/3$ ($R\gg I$) as compared to $\alpha_L=\sigma_Y^2 I$ for uniform flows, as already discussed above. This is a general result, independent of e and of the shape of ρ_Y.

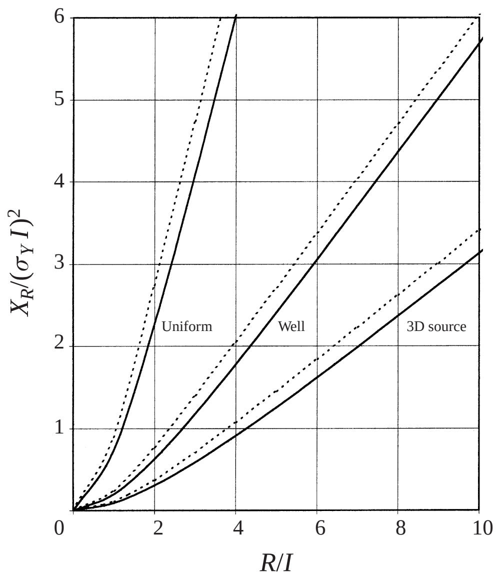

FIGURE 7. Trajectory variance X_R for a well flow (43), (44), for a three-dimensional source (53), (54), and for a uniform flow, for Gaussian (dotted line) and exponential (full line) covariances (infinite Pe).

The above simple result, namely $\alpha_R^{(app)}/(\sigma_Y^2 I) = 1/3$, can be easily extended to the case of a point source in three dimensions, which may be an approximate representation of a short, partially penetrating well. We consider flow in a three-dimensional isotropic medium for which

$$U = \langle V_r \rangle = \frac{Q}{4\pi n r^2} \tag{46}$$

and the mean radial trajectory is

$$R = \langle X_r \rangle = \left(\frac{3Qt}{4\pi n} \right)^{1/3}. \tag{47}$$

The trajectory fluctuation $X_r'(t)$ satisfies the equation

$$\frac{\mathrm{d}X_r'}{\mathrm{d}t} = u_r(R) - \frac{2X_r'}{3t} \tag{48}$$

whose solution is given by

$$X_r'(R) = \frac{4\pi n}{QR^2} \int_0^R r^4 V_1'(r)\,\mathrm{d}r. \tag{49}$$

The variance of the particle trajectory is obtained now as

$$X_{rr}(R) = \frac{16\pi^2 n^2}{Q^2 R^4} \int_0^R \int_0^R (r'r'')^4 u_{rr}(r', r'')\,\mathrm{d}r'\mathrm{d}r''. \tag{50}$$

By a similar approximation, i.e. retaining only the first term in u_{rr} (24) and with $E_r^{(0)} = Q/(4\pi K_G r^2)$, we get now

$$X_R(R) = \frac{2\sigma_Y^2 R}{5} \int_0^R \left(1 - \frac{5r}{2R} + \frac{5r^2}{3R^2} - \frac{r^5}{6R^5} \right) \rho(r)\,\mathrm{d}r. \tag{51}$$

The asymptotic longitudinal 'dispersivity' $\alpha_R^{(app)} = \lim_{R\to\infty}(1/2)\,\mathrm{d}X_R/\mathrm{d}R$ becomes

$$\alpha_R^{(app)} = \lim_{R\to\infty} \frac{\sigma_Y^2}{5} \int_0^R \left(1 - \frac{5r^2}{3R^2} + \frac{2r^5}{3R^5}\right) \rho(r)\, dr = \frac{\sigma_Y^2 I}{5} = \frac{\alpha_L}{5}. \quad (52)$$

The expressions (51) and (52) yield

$$\frac{X_R}{I^2\sigma_Y^2} = \frac{4R'}{5\pi}\left[\left(1 + \frac{5}{6R'^2}\right)\pi^{1/2}\mathrm{erf}\,(R') - \frac{5}{2R'} - \frac{1}{3R'^5} + \left(\frac{1}{R'} + \frac{1}{3R'^3} + \frac{1}{3R'^5}\right)\exp\,(-R'^2)\right] \quad (R' = \pi^{1/2}R/2I) \quad (53)$$

for the Gaussian ρ_Y and

$$\frac{X_R}{I^2\sigma_Y^2} = \frac{2\overline{R}}{5}\left[1 - \frac{5}{2\overline{R}} + \frac{10}{3\overline{R}^2} - \frac{20}{\overline{R}^5} + \left(1 + \frac{2}{\overline{R}} + \frac{2}{\overline{R}^2}\right)\frac{10\exp\,(-\overline{R})}{\overline{R}^3}\right] \quad (54)$$

for the exponential ρ_Y. Both trajectory variances X_R (53), (54) for a three-dimensional source are shown in figure 7.

These results are easily generalized for a source in anisotropic media. Thus, for axisymmetric heterogeneity all expressions hold after the substitution $I \to eI/(e^2\cos^2\varphi + \sin^2\varphi)^{1/2}$ where φ is the angle between the mean trajectory and the plane of isotropy.

The large time limit of $\alpha_R^{(app)} = \lim_{R\to\infty}(1/2U)\,(\mathrm{d}X_R/\mathrm{d}t)$ is found in both cases to be given by $\alpha_R^{(app)}/(\sigma_Y^2 I) = 1/5$, a further reduction compared to well flow. This large time limit of α_R can be written for a space of d dimensions in an unified form as

$$\lim_{R\to\infty}\alpha_R^{(app)} = \lim_{t\to\infty}\alpha_R^{(app)} = \frac{\sigma_Y^2 I}{2d-1} = \lim_{t\to\infty}\frac{\alpha_L}{2d-1} \quad (d \geqslant 1). \quad (55)$$

Note that in (55) d is the dimensionality of the mean flow.

Again, using the definition of $\alpha_R^{(eq)}$ of § 4.4 and comparing with Gelhar & Collins's, (1971) solution for a homogeneous medium leads to the same result, namely that asymptotically $\alpha_R^{(eq)} = \alpha_L = \sigma_Y^2 I$.

5. Summary and discussion

The problem investigated here is that of spreading of a solute plume injected by a fully penetrating well in a heterogeneous formation and advected by the steady fluid velocity. In a homogeneous medium such a thin plume propagates by advection as a cylinder of radius $R(t)$ and spreads around it by the effect of longitudinal pore-scale dispersion. In the heterogeneous medium the plume spreads around the mean front $r = R$ due to the fluctuations of the macroscopic velocity that are caused in turn by the spatial variability of the permeability. For the large Péclet numbers of interest in applications, the rate of spreading due to heterogeneity is much larger than the one stemming from longitudinal pore-scale dispersion, which can be neglected altogether. In contrast, pore-scale dispersion may have an appreciable impact due to transverse mixing. The spreading of the plume is analysed with the aid of the second spatial moment S_{rr}, which under ergodic conditions is equal to the trajectory variance X_{rr}. In field tests (e.g. Molz *et al.* 1986; Yeh *et al.* 1995), the detection of the plume is carried out by piezometers parallel to the well. In the simplest approach, concentration is averaged over the vertical by measuring it after mixing in the piezometer. Assuming ergodic conditions, i.e. thickness of formation much larger than the vertical correlation scale, the spreading in the breakthrough measured by such a piezometer and characterized by the second temporal moment is directly related to X_{rr} (see e.g. Cvetkovic & Dagan 1994 for a similar analysis in uniform flow). In more elaborate experiments, concentration is measured with the aid of multilevel samplers at a large number of points along the piezometer. Then the breakthroughs at different depths may be used in order to determine the statistics of the arrival times which can be related again to X_{rr}.

After making a few simplifying assumptions, our analysis is based on approximating X_{rr} by X_R which in turn results from the relationships

$$\frac{\mathrm{d}X'_r}{\mathrm{d}t} = u_r(R, 0, X_{d3}) + X'_r \frac{\mathrm{d}U(R)}{\mathrm{d}R}, \quad \frac{\mathrm{d}R}{\mathrm{d}t} = U(R), \quad u_r = U(R)\, Y'(\boldsymbol{x}), \tag{56}$$

where it should be recalled that U and u_r are the radial velocity mean and fluctuation, respectively, Y' is the log-conductivity fluctuation and X_{d3} is the trajectory fluctuation in the vertical direction due to transverse pore-scale dispersion. This approximation is supposed to apply to formations of anisotropic heterogeneity of, say, $e < 0.2$, which is the case for most sedimentary formations, and it leads to the simple expressions for X_R (35), (36).

It is customary in practice to characterize the heterogeneity-induced dispersion in mean uniform flow by a macrodispersion coefficient and by a macrodispersivity that are related to X_{rr} in a similar manner to the definition of Fickian diffusion coefficients. These coefficients are convenient for comparing dispersion in radial flow with that prevailing in mean uniform flow or with pore-scale dispersion in a homogeneous medium. The definition of macrodispersivity in transport by mean non-uniform flow is not straightforward. We define two asymptotic, far from the well, longitudinal macrodispersivities: the apparent $\alpha_R^{(app)}$ and the equivalent $\alpha_R^{(eq)}$ ones. The first characterizes the rate of change of the second spatial moment in a manner similar to the uniform flow case. The equivalent macrodispersivity replaces the longitudinal pore-scale dispersivity in radial flow in a homogeneous medium, such as to match the rate of spreading in the heterogeneous medium.

Our main finding is that the asymptotic, for large R/I, apparent macrodispersivity in radial well flow is constant and smaller than that in mean uniform flow (see figures 1 and 6) by a factor of 3 for well flow and by a factor of 5 for source flow. This important finding has the following kinematical interpretation. The asymptotic dispersivity is simply related to the Lagrangian macroscale, which in turn is a measure of the time for which the velocities of two particles are correlated. Roughly speaking, the velocities of two particles injected at a time interval T at the source become uncorrelated if T is larger than the time required for a particle to move over a heterogeneity integral scale I at the mean velocity U. While U is constant in uniform flow, it is large near the source and drops quickly with distance for radial flow, and the net effect is a reduction of the Lagrangian macroscale and even of the macrodispersivity, which is obtained by multiplication with U at time T. A similar effect is observed for homogeneous media and for a longitudinal pore-scale dispersion coefficient that is proportional to the fluid velocity (Gelhar & Collins 1971). The explanation there is that the time spent in the high-velocity zone adjacent to the well is a small part of the total travel time.

In contrast, the equivalent macrodispersivity in radial flow is equal to that in mean uniform flow far from the well. This finding, in agreement with the similar one for the equivalent permeability, stems from the slow spatial variation of the velocity field far from the well.

The present study was carried out in the framework of a joint project with Institut de Mécanique des Fluides, Strasbourg University. The support of the Israel Ministry of Science and Technology and of the French Ministère de l'Education, de l'Enseignement Supérieur et de la Recherche is kindly acknowledged. We are grateful to one of the anonymous reviewers for his constructive comments.

Appendix A. Derivation of X_{rr} for radial flow in a medium of Gaussian log-conductivity correlation

In order to assess the accuracy of approximation of § 4.3, we evaluate here the complete expression of X_{rr} for infinite Pe.

The σ_Y-order head field is given by the solution of (8)

$$H^{(1)}(\boldsymbol{x}) = -\int E_r^{(0)}(r') \frac{\partial Y'(\boldsymbol{x}')}{\partial r'} G(\boldsymbol{x}-\boldsymbol{x}')\, \mathrm{d}\boldsymbol{x}' \tag{A 1}$$

where $G = 1/[4\pi|\boldsymbol{x}-\boldsymbol{x}'|]$.

The main difficulty in evaluating u_{rr} (24) stems from the covariances in the last three terms of (24). They can be written as follows by using (23), (A 1):

$$C_{E_rY}(r', r'') = \sigma_Y^2 \iiint E_r^{(0)}(r) \frac{\partial \rho_Y(\boldsymbol{x} - r''\boldsymbol{i}_1)}{\partial r} \frac{\partial G(r'\boldsymbol{i}_1 - \boldsymbol{x})}{\partial r'}\, \mathrm{d}\boldsymbol{x}, \tag{A 2}$$

$$C_{E_rE_r}(r', r'') = \sigma_Y^2 \iiint \iiint E_r^{(0)}(x_r)\, E_r^{(0)}(y_r) \frac{\partial^2 \rho_Y(\boldsymbol{x}-\boldsymbol{y})}{\partial x_r \partial y_r} \frac{\partial G(r'\boldsymbol{i}_1 - \boldsymbol{x})}{\partial r'} \frac{\partial G(r''\boldsymbol{i}_1 - \boldsymbol{y})}{\partial r''}\, \mathrm{d}\boldsymbol{x}\, \mathrm{d}\boldsymbol{y}, \tag{A 3}$$

where $\boldsymbol{i}_1$ is the unit vector along the axis x_1, $x_r = (x_1^2 + x_2^2)^{1/2}$ and similarly for y_r.

As mentioned before, in the case of uniform flow, closed-form analytical expressions could be obtained for the similar terms of u_{11} (14) for exponential or Gaussian isotropic ρ_Y, whereas one quadrature is needed to evaluate them for axisymmetric anisotropy. In contrast, no integration could be performed analytically in (A 2), (A 3) and this underscores the complexity of radial flow, the simplifying assumptions enumerated above notwithstanding.

We start with the correlations C_{E_rY} (A 2) and $C_{E_rE_r}$ (A 3) involved in the velocity covariance (24). Introducing cylindric variables one gets

$$C_{E_rY}(\tilde{r}', \tilde{r}'') = \frac{\sigma_Y^2 Q}{8\pi^{3/2} K_G I} \int_0^\infty \int_0^{2\pi} \int_{-\infty}^{\infty} \exp\left(-r^2 + 2r\tilde{r}''\cos\theta - \tilde{r}''^2 - z^2 e^{-2}\right) \times \frac{(r - \tilde{r}''\cos\theta)(\tilde{r}' - r\cos\theta)}{(\tilde{r}'^2 - 2r\tilde{r}'\cos\theta + r^2 + z^2)^{3/2}}\, \mathrm{d}r\, \mathrm{d}\theta\, \mathrm{d}z, \tag{A 4}$$

$$C_{E_1E_1}(\tilde{r}', \tilde{r}'') = \frac{\sigma_Y^2 Q^2}{128\pi^3 K_G^2 I^2} \int_0^{2\pi}\int_0^{2\pi}\int_0^\infty\int_0^\infty\int_{-\infty}^\infty\int_{-\infty}^\infty \Lambda \exp\left[-\zeta - (z' - z'')^2 e^{-2}\right] \times \frac{(\tilde{r}' - \bar{r}'\cos\theta')(\tilde{r}'' - \bar{r}''\cos\theta'')}{\left[(\xi^2 + z'^2)(\eta^2 + z''^2)\right]^{3/2}}\, \mathrm{d}\theta'\mathrm{d}\theta''\mathrm{d}\bar{r}'\mathrm{d}\bar{r}''\mathrm{d}z'\mathrm{d}z'', \tag{A 5}$$

$$\Lambda = 2(\bar{r}' - \bar{r}'' \cos(\theta' - \theta''))\,(\bar{r}'' - \bar{r}' \cos(\theta' - \theta'')) + \cos(\theta' - \theta''),$$

$$\xi^2 = \tilde{r}'^2 + \bar{r}'^2 - 2\tilde{r}'\bar{r}' \cos(\theta' - \theta''),$$

$$\eta^2 = \tilde{r}''^2 + \bar{r}''^2 - 2\tilde{r}''\bar{r}'' \cos(\theta' - \theta''),$$

$$\zeta = \bar{r}'^2 + \bar{r}''^2 - 2\bar{r}'^2\bar{r}''^2 \cos(\theta' - \theta''),$$

where $\tilde{r}' = \pi^{1/2} r'/2I$ and $\tilde{r}'' = \pi^{1/2} r''/2I$.

Substituting (A 4) and (A 5) into (24) and the result in (29) yields $X_{rr} = X_R + X_{rr}^{E_rY} + X_{rr}^{E_rE_r}$ where X_R is given by (42) and

$$X_{rr}^{E_rY}(R') = \frac{4\sigma_Y^2 I^2}{\pi^2 R'^2} \int_0^\infty \int_0^{2\pi} \int_{-\infty}^\infty \exp\left(-z^2 e^{-2}\right) \Psi(r, R', \theta) F(r, R', \theta, z)\, \mathrm{d}r \mathrm{d}\theta \mathrm{d}z, \qquad (\mathrm{A}\,6)$$

$$X_{rr}^{E_rE_r}(R') = \frac{\sigma_Y^2 I^2}{2\pi^3 R'^2} \int_0^{2\pi} \int_0^{2\pi} \int_0^\infty \int_0^\infty \int_{-\infty}^\infty \int_{-\infty}^\infty \Lambda \exp\left[-\zeta - \frac{(z' - z'')^2}{e^2}\right]$$
$$\times F(\bar{r}', R', \theta', z') F(\bar{r}'', R', \theta'', z'')\, \mathrm{d}\theta' \mathrm{d}\theta'' \mathrm{d}\bar{r}' \mathrm{d}\bar{r}'' \mathrm{d}z' \mathrm{d}z'', \qquad (\mathrm{A}\,7)$$

$$\Psi(r, R, \theta) = \tfrac{1}{2}\left[\left(R\cos\theta - r\sin^2\theta\right) \exp\left(-R^2 + 2rR\cos\theta - r^2\right) + r\sin^2\theta \exp\left(-r^2\right)\right]$$
$$+ \tfrac{1}{4}\pi^{1/2}\left(2r^2\sin^2\theta - 1\right)\cos\theta\, [\,\mathrm{erf}\,(R - r\cos\theta)$$
$$+ \mathrm{erf}\,(r\cos\theta)]\, \exp\left(-r^2\sin^2\theta\right),$$

$$F(r, R, \theta, z) = \overline{F}(r, R, \theta, z) - \overline{F}(r, 0, \theta, z),$$

$$\overline{F}(r, R, \theta, z) = 2N + 2r\cos\theta \ln\left[R - r\cos\theta + N\right] - \frac{R^2}{N},$$

$$N = \left(R^2 - 2rR\cos\theta + r^2 + z^2\right)^{1/2},$$

with $R' = \pi^{1/2} R/2I$.

Similarly to the uniform flow, the covariances (A 2), (A 3) are $O(e)$ and can be expanded in a power series for small e. The leading-order term can be obtained directly by approximating ρ_Y as

$$\rho_Y(\boldsymbol{x}) = 2\,\rho_{Yh}(r)\,\delta(x_3/I_v), \quad \rho_{Yh}(r) = \rho_Y(r, 0, 0), \qquad (\mathrm{A}\,8)$$

i.e. replacing the vertical autocorrelation by a 'white noise' approximation. As a result, the number of integrations in (A 2), (A 3) is reduced by one. This approximation was employed by Fiori *et al.* (1998) to investigate the variation of u_{rr} along the radial and vertical directions. Thus for highly anisotropic media (small e) substituting (A 8) simplifies (A 6) and (A 7) to

$$X_{rr}^{E_rY}(R) = \frac{4e\sigma_Y^2 I^2}{\pi^{3/2} R'^2} \int_0^\infty \int_0^{2\pi} \Psi(r, R', \theta) F(r, R', \theta, 0)\, \mathrm{d}r\, \mathrm{d}\theta, \qquad (\mathrm{A}\,9)$$

$$X_{rr}^{E_rE_r}(R) = \frac{e\sigma_Y^2 I^2}{2\pi^{5/2} R'^2} \int_0^{2\pi} \int_0^{2\pi} \int_0^\infty \int_0^\infty \int_{-\infty}^\infty \Lambda \exp(-\zeta)$$
$$\times F(\bar{r}', R', \theta', z) F(\bar{r}'', R', \theta'', z)\, \mathrm{d}\theta' \mathrm{d}\theta'' \mathrm{d}\bar{r}' \mathrm{d}\bar{r}'' \mathrm{d}z. \qquad (\mathrm{A}\,10)$$

These expressions were used in order to compute X_{rr} and depict the curves of figure 4 that served the discussion in the main text.

Appendix B. Spatial moments of a finite plume

In the main text we have derived the radial spatial moment of a thin plume. The extension of the results for a plume of finite initial thickness is straightforward and is given here. Thus the transport initial condition is now

$$C = C_0 \quad \text{for} \quad t = 0 \quad \text{and} \quad \boldsymbol{x} \in V_0,$$

where V_0 is a cylinder of radius r_0 surrounding the well.

The solute mass, which is preserved, is given by $M = \int nC\,\mathrm{d}\boldsymbol{x} = \pi r_0^2 L_3 n C_0$ whereas the second spatial moment is defined by the general relationship (7). In the present case it becomes

$$S_{rr}(t) = \langle S_{rr}(t)\rangle = \frac{2}{r_0^2}\int_0^{r_0}\left[\langle X_r\rangle^2 - S_r^2 + \langle X_r'^2\rangle\right] a\,\mathrm{d}a.$$

Recall that $\langle X_r(t;a)\rangle = a + \int_0^t U(t')\,\mathrm{d}t'$ and the centroid coordinate in the present case is given by $S_r = 2R^3/3/r_0^2[(1 + r_0^2/R^2)^{3/2} - 1]$, while $R = \langle X_r(t;0)\rangle = (Qt/\pi n)^{1/2}$.

Let $S_{rr} = S_{rr}^{(hm)} + S_{rr}^{(ht)}$ where

$$S_{rr}^{(hm)} = \frac{2}{r_0^2}\int_0^{r_0}[\langle X_r\rangle^2 - R_r^2]\,a\,\mathrm{d}a = R^2 + \frac{r_0^2}{2} - R_r^2$$

is the contribution to the spatial moment due to the non-uniformity of the mean flow. In contrast

$$S_{rr}^{(ht)} = \frac{2}{r_0^2}\int_0^{r_0}\langle X_r'^2\rangle\,a\,\mathrm{d}a = X_{rr}(t)$$

is entirely due to the formation heterogeneity. One can define an asymptotic dispersion coefficient by $\alpha_{rr} = \lim_{t\to\infty}(1/2U)\,\mathrm{d}S_{rr}/\mathrm{d}t$ which will be equal to the one derived in the main text for a thin plume, stemming from heterogeneity and pore-scale dispersion, and an apparent one related to the stretching effect of the mean flow. Thus

$$D_{rr} = \frac{1}{2}\frac{\mathrm{d}S_{rr}}{\mathrm{d}t} = \frac{1}{2}\frac{\mathrm{d}S_{rr}^{(hm)}}{\mathrm{d}t} + \frac{1}{2}\frac{\mathrm{d}S_{rr}^{(ht)}}{\mathrm{d}t} = D_{rr}^{(hm)} + D_{rr}^{(ht)}$$

where

$$D_{rr}^{(hm)} = \frac{1}{2}\frac{\mathrm{d}S_{rr}^{(hm)}}{\mathrm{d}R}\frac{\mathrm{d}R}{\mathrm{d}t} = -\frac{Q}{2\pi n}\left\{1 - \frac{4R^4}{3r_0^4}\left[\left(1 + \frac{R^2}{r_0^2}\right)^{3/2} - 1\right]\left[\left(1 + \frac{r_0^2}{R^2}\right)^{1/2} - 1\right]\right\}$$

so that for small r_0/R

$$D_{rr}^{(hm)} = -\frac{r_0^4}{48R^3}\frac{\mathrm{d}R}{\mathrm{d}t}.$$

The trajectory fluctuation is given by (29) after replacing the integral limits from a to R, i.e.

$$X_{rr}(R;a) = \left(\frac{2\pi n}{QX_r}\right)^2\int_a^{X_r}\int_a^{X_r}(r'r'')^2 u_{rr}(r',r'')\,\mathrm{d}r'\mathrm{d}r''$$

where $X_r = \left(R^2 + a^2\right)^{1/2}$. For $r_0/R \to 0$ we see that X_{rr} tends to X_{rr} (29) of the main paper. The radial dispersion is given now by

$$D_{rr}^{(ht)}(R;a) = \frac{2}{r_0^2}\int_0^{r_0}\left(\frac{2\pi n}{QX_r}\right)^2\int_a^{X_r}\int_a^{X_r}(r'r'')^2 u_{rr}(r',r'')\,a\,\mathrm{d}r'\mathrm{d}r''\mathrm{d}a$$

and for our approximation, $u_{rr}(r',r'') \simeq U(r')U(r'')\sigma_Y^2\rho_Y(r'-r'')$, it tends to $U\alpha_R$ (45) for $t\to\infty$ and at the same limit $r_0/R\to 0$.

It is seen that the apparent dispersive effect associated with the mean flow stretching is very small compared with that resulting from heterogeneity. Hence, the results obtained in the main text for a thin plume can be adopted for a finite one as well.

REFERENCES

Adams, E. E. & Gelhar, M. A. 1992 Field study of dispersion in a heterogeneous aquifer x2. Spatial moments analysis. *Water Resour. Res.* **28**, 3293–3307.

Bellin, A. & Salandin, P. & Rinaldo, A. 1992 Simulation of dispersion in heterogeneous porous formations: statistics, first-order theories, convergence of computations. *Water Resour. Res.* **28**, 2211–2228.

Chen, C. S. 1987 Analytical solution for radial dispersion with Cauchy Boundary at injection well. *Water Resour. Res.* **23**, 1217–1224.

Chin, D. A. 1997 An assessment of first-order stochastic dispersion theories in porous media. *J. Hydrol.* **190**, 53–73.

Cvetkovic, V. & Dagan, G. 1994 Transport of kinetically sorbing solute by steady random velocity in heterogeneous porous formations. *J. Fluid Mech.* **265**, 189–215.

Dagan, G. 1971 Perturbation solutions of the dispersion equation in porous mediums. *Water Resour. Res.* **7**, 135–142.

Dagan, G. 1982 Analysis of flow through heterogeneous random aquifers 2. Unsteady flow in confined formations. *Water Resour. Res.* **18**, 1571–1585.

Dagan, G. 1984 Solute transport in heterogeneous porous formations. *J. Fluid Mech.* **145**, 151–177.

Dagan, G. 1987 Theory of solute transport by groundwater. *Ann. Rev. Fluid Mech.* **19**, 183–215.

Dagan, G. 1989 *Flow and Transport in Porous Formations*. Springer.

Fiori, A. 1996 Finite Peclet extension of Dagan's solutions to transport in anisotropic heterogeneous formations. *Water Resour. Res.* **32**, 193–198.

Fiori, A., Indelman, P. & Dagan G. 1998 Steady flow toward wells in heterogeneous formations: Correlation structure of flow variables. *Water Resour. Res.* **34**, 699–708.

Gelhar, L. J. & Axness, C. L. 1983 Three-dimensional stochastic analysis of macrodispersion in aquifers. *Water Resour. Res.* **19**, 161–180.

Gelhar, L. W. & Collins, M. A. 1971 General analysis of longitudinal dispersion in nonuniform flow. *Water Resour. Res.* **7**, 1511–1521.

Hsieh, P. A. 1986 A new formula for the analytical solution of the radial dispersion problem. *Water Resour. Res.* **22**, 1597–1605.

Indelman, P. 1996 Averaging of unsteady flows in heterogeneous media of stationary conductivity. *J. Fluid Mech.* **310**, 39–60.

Indelman, P. & Abramovich, B. 1994 Nonlocal properties of nonuniform averaged flows in heterogeneous media. *Water Resour. Res.* **30**, 3385–3393.

Indelman, P., Fiori, A. & Dagan, G. 1996 Steady flow toward wells in heterogeneous formations: mean head and equivalent conductivity. *Water Resour. Res.* **32**, 1975–1983.

Molz, F. J., Guven, O., Melville, J. G., Crocker, R. D. & Matteson, K. T. 1986 Performance, analysis, and simulation of a two-well tracer test at the mobile site. *Water Resour. Res.* **22**, 1031–1037.

Naff, R. L. 1990 On the nature of dispersive flux in saturated heterogeneous porous media. *Water Resour. Res.* **26**, 1013–1026.

Neuman, S. P. & Orr, S. 1993 Prediction of steady state flow in nonuniform geologic media by conditional moments: exact nonlocal formalism, effective conductivities, and weak approximation. *Water Resour. Res.* **29**, 341–364.

Shvidler, M. I. 1966 The source-type solution of the problem of unsteady flow in random porous media. *Izv. Akad. Nauk USSR Mekh. Zhidk. Gaza* **4**, 137–141 (in Russian) (Engl. transl. *Fluid Dyn.* 95–98).

Shvidler, M. I. 1985 *Stochastic Hydrodynamics of Porous Media.* Nedra, Moscow (in Russian).

Valocchi, A. J. 1986 Effect of radial flow on deviation from local equilibrium during sorbing solute transport through homogeneous soils. *Water Resour. Res.* **22**, 1693–1701.

Yeh, T.-C. J., Mas-Pla, J., Williams, T. M. & McCarthy, J. F. 1995 Observation and three-dimensional simulation of chloride plumes in a sandy aquifer under forced-gradient conditions. *Water Resour. Res.* **31**, 2141–2157.